

Published in final edited form as:

*Small*. 2009 August 17; 5(16): 1862–1868. doi:10.1002/smll.200900389.

## Drug/Dye-Loaded, Multifunctional Iron Oxide Nanoparticles for Combined Targeted Cancer Therapy and Dual Optical/MR-Imaging\*\*

**Dr. Santimukul Santra,**

Nanoscience Technology Center, Chemistry Department, Burnett School of Biomedical Sciences, College of Medicine, University Of Central Florida, 12424 Research Parkway, Suite 400, Orlando, FL 32826 (USA)

**Mr. Charalambos Kaittanis,**

Nanoscience Technology Center, Chemistry Department, Burnett School of Biomedical Sciences, College of Medicine, University Of Central Florida, 12424 Research Parkway, Suite 400, Orlando, FL 32826 (USA)

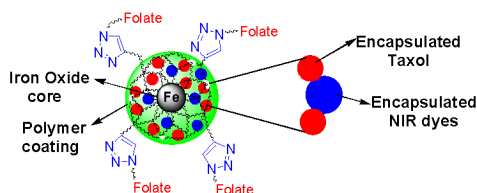
**Dr. Jan Grimm,** and

Department of Radiology, Memorial Sloan Kettering Cancer Center, New York, NY

**Dr. J. Manuel Perez\***

Nanoscience Technology Center, Chemistry Department, Burnett School of Biomedical Sciences, College of Medicine, University Of Central Florida, 12424 Research Parkway, Suite 400, Orlando, FL 32826 (USA)

### Abstract



A biocompatible, multimodal and theranostic functional IONPs was synthesized using a novel waterbased method and exerted excellent properties for targeted cancer therapy, optical and magnetic resonance imaging (MRI). For the first time, a facile, modified solvent diffusion method is used for the co-encapsulation of both an anti-cancer drug and near infrared dyes. The resulting folate-derivatized theranostics nanoparticles could allow for targeted optical/MR-imaging and targeted killing of folate expressing cancer cells.

\*\*This work was supported by NIH grants CA101781 and GM084331 to JMP. We thank Dr Korey Sorge at Florida Atlantic University for SQUID studies. Technical services provided by the MSKCC Small Imaging Core Facility from NIH Small Animal Imaging Research Program (SAIRP) Grant No R24 CA83084 and NIH Grant No P30 CA08748 are acknowledged. This work was also supported in part by R25 CA096945-05 (JG)

\*jmperez@mail.ucf.edu Phone: 407-882-2843.

Supporting information for this article is available on the WWW under <http://www.small-journal.org> or from the author.

## Keywords

magnetic nanoparticles; click chemistry; targeted drug delivery; magnetic resonance imaging; drug release

Superparamagnetic iron oxide nanoparticles with dual imaging and therapeutic capabilities hold great promise for the non-invasive detection and treatment of tumors.[1] When conjugated with tumor-specific targeting ligands, these multifunctional nanoparticles can be used to specifically deliver anti-cancer drugs to tumors, thereby minimizing severe side effects.[2] To meet the demand for the rapid development and potential clinical application of targeted anti-cancer nanotherapies, it is desirable to introduce optical (fluorescent) imaging capabilities to these nanoparticles to facilitate non-invasive assessment of drug homing and efficacy. This is often achieved by crosslinking the polymeric coating surrounding the nanoparticle and functionalizing its surface with amine or carboxyl groups that are then used to conjugate fluorescent dyes and drugs.[3] This approach to introduce multimodality (magnetic and fluorescent)[4] and multifunctionality (imaging and therapeutic)[5] to iron oxide nanoparticles (IONPs), although widely used, often compromises the solubility of the nanoparticles in aqueous media and reduces the number of available functional groups that otherwise could be used to attach ligands for targeting applications.

Herein, we report the co-encapsulation of a lipophilic near infrared (NIR) dye and an anti-cancer drug within hydrophobic pockets in the polymeric matrix of polyacrylic acid (PAA)-coated IONPs (PAA-IONPs) for combined optical imaging, MRI detection and targeted cancer therapy. Our water-based and green chemistry approach to synthesize these nanoparticles have five key components (a) an encapsulated chemotherapeutic agent (Taxol) for cancer therapy, (b) surface functionality (folic acid ligand) for cancer targeting, (c) “click”-chemistry-based conjugation of targeting ligands, (d) an encapsulated NIR dye for fluorescent imaging capabilities and (e) a superparamagnetic iron oxide core for magnetic resonance imaging (MRI).

Specifically, our synthetic procedure differs from the previously reported methods in that the polymer is not present during the initial nucleation process.[6–8] Instead, the polyacrylic acid is added at a later stage. This “step-wise” process, as opposed to the “in-situ” process, allows for the formation of stable, disperse and highly crystalline superparamagnetic iron oxide nanocrystals coated with PAA, (1, Scheme 1). The successful coating with PAA was confirmed by the presence of a negative zeta-potential ( $\zeta = -48$  mV) and via FT-IR analysis (Supporting Information 5). We then hypothesized whether a hydrophobic dye could be encapsulated within the hydrophobic pockets in the PAA coating, generating multimodal IONPs with dual magnetic and fluorescent properties. As a proof-of-principle, we have encapsulated two lipophilic fluorescent dyes (DiI or DiR) (2, Scheme 1) using a modified solvent diffusion method.[9] These dialkylcarbocyanine fluorophores (DiI, DiR) are widely used in biomedical applications to label cell membranes and were selected because of their high extinction coefficients ( $\epsilon > 125,000$  cm<sup>-1</sup>M<sup>-1</sup>) and high fluorescence in hydrophobic environments.[9] The long chain dialkylcarbocyanine dye, DiR, is of particular importance since it has an excitation/emission near the infrared region (751/780), suitable for *in vivo* imaging.

Next, the IONP 1 was functionalized to yield a propargylated nanoparticle (3, Scheme 1), which was later used to generate a multimodal folate-derivatized nanoparticle (4, Scheme 1) via highly selective 1,3-dipolar cycloaddition reaction (“click” chemistry).[10] Thus, the water-soluble carbodiimide EDC, [1-ethyl-3-(3-dimethylaminopropyl) carbodiimide

hydrochloride] was utilized to prepare the propargylated IONP (3, Scheme 1), which is an important synthon for the synthesis of a library of functional IONPs via “click” chemistry. The presence of a weak ‘C≡C’ band at  $2265\text{ cm}^{-1}$  in the FT-IR spectrum of these nanoparticles confirmed the presence of a propargyl (triple bond) group (Supporting Information 6). As a model system, we conjugated the nanoparticle 3 with an azide-functionalized folic acid[11] analog (Supporting Information 1 and 2) via “click” chemistry. The resulting folate-decorated IONPs are soluble in aqueous media and can encapsulate lipophilic fluorescent dyes. The presence of folic acid and dye in these multimodal folate-derivatized nanoparticles (4, Scheme 1) was confirmed through various spectrophotometric studies (Supporting Information 7, 8 and 9). Furthermore, a hydrophobic anti-cancer drug (Taxol) was encapsulated to yield a theranostic (therapeutic and diagnostic) nanoparticle with dual imaging and therapeutic properties (5, Scheme 1). These functional IONPs (1–5) were highly stable in aqueous solutions, as their magnetic relaxivity ( $R_2$ ), hydrodynamic diameter (D) and polydispersity index (PDI) remained unaffected over a long period of time (Supporting Information 3). Therefore, the versatility of our method allows the generation of a small library of multifunctional, multimodal and targetable IONPs.

Dynamic light scattering (DLS) studies of the functional PAA-IONP (2) confirmed the presence of stable and monodispersed nanoparticles with a hydrodynamic diameter of 90 nm (Figure 1A), while TEM experiments revealed an iron oxide core of 8 nm (Inset: Figure 1A; Supporting Information 4). These measurements suggest the formation of a thick polymeric coating (~40 nm) around the iron oxide core, which plays a key role in the encapsulation of hydrophobic guest molecules. FT-IR analysis further confirmed the presence of the PAA coating and carboxylic acid groups on 1, as well as the corresponding surface propargyl groups on nanoparticle 3 (Supporting Information 5 and 6). Magnetic hysteresis loops (Figure 1B) corroborated the superparamagnetic nature of the nanoparticles, while water relaxation measurements using a 0.47T Bruker’s Minispec relaxometer indicated the presence of magnetic IONPs with high water relaxation ( $R_1 = 53\text{ s}^{-1}\text{ mM}^{-1}$ ,  $R_2 = 202\text{ s}^{-1}\text{ mM}^{-1}$ ). The incorporation of a hydrophobic dye into 1 was done using a modified solvent diffusion method.[9] Specifically, a solution of DiI in DMF ( $0.1\text{ }\mu\text{g}/\mu\text{L}$ ) was added drop-wise to a stirring aqueous nanoparticle suspension (4.5 mL and  $[\text{Fe}] = 1.1\text{ mg}/\text{mL}$ ). The slow addition of the dye solution allows for the rapid diffusion of DMF into the aqueous medium, causing the dye to become encapsulated in the hydrophobic microdomains of the PAA coating. The presence of an absorption maximum at 555 nm in the UV/Vis spectrum (Supporting Information 8a) and a corresponding fluorescence emission peak at 595 nm (Figure 1C) confirmed the presence of DiI in the nanoparticle. Furthermore, the encapsulation of DiI was confirmed by the presence of a 14 nm red-shift in the fluorescence intensity maximum of the DiI-encapsulating PAA-IONP, as compared to the free DiI (581 nm, Figure 1D). Similar red-shifts have been previously reported in other systems, indicating an interaction of the fluorescent guest molecule with the electronic environment of the encapsulating pocket.[12] Next, we encapsulated both DiI and Taxol to the folate-conjugated nanoparticle for dual cellular imaging and targeted cancer therapy. To synthesize such nanoparticle (5), a DMF solution containing DiI ( $0.1\text{ }\mu\text{g}/\mu\text{L}$ ) and Taxol ( $0.05\text{ }\mu\text{g}/\mu\text{L}$ ) was added to a stirring solution of folate-derivatized PAA-IONPs (3a, Supporting Information 1). Since the dye and the drug are hydrophobic, we expected both molecules to become encapsulated. The encapsulation of Taxol was confirmed through fluorescence spectroscopy (Supporting Information 10). Furthermore, the amount of dye, folic acid and Taxol molecules per nanoparticle was calculated, as previously described [13] (Table 1). These dye- encapsulating PAA-IONPs were highly stable in aqueous solutions for more than a year, without significant reduction in the fluorescence emission of the encapsulated dyes. Additionally, no leaching of the encapsulated dye from the nanoparticle occurred, as no precipitation of the dye was observed after prolonged storage in PBS, pH 7.4.

To evaluate the potential biomedical applications of the DiI-encapsulating IONPs (2, 3, 4 and 5, 1.1 mg/mL), we assessed their potential cytotoxicity, via the MTT assay (Figure 2). Therefore, we examined the *in vitro* differential cytotoxicity of carboxylated (COOH, 2), propargylated (PROPARGYL, 3), folate-decorated (FOLATE, 4), folate-decorated and taxol-encapsulating IONPs (TAXOL, 5), using lung carcinoma (A549, 2,500 cells/well) (Figure 2A) and cardiomyocyte cell lines (H9c2, 2,500 cells/well) (Figure 2B). Carboxylated, propargylated and folate-conjugated IONPs exhibited nominal cytotoxicity (less than 3% compared to the control) towards both cell lines after a 3 h incubation. On the other hand, incubation with the folate-decorated and taxol-carrying IONPs (5) resulted in an 80% reduction in the viability of the lung carcinoma (A549) cell line. In contrast, no significant reduction in cell viability was observed when cardiomyocytes (H9c2) which do not overexpress the folate receptor [14] were incubated with 5. These results demonstrate that nanoparticles 1–4 were not toxic to either A549 or H9c2 cells, hence these nanoparticles can be used as effective multimodal imaging agents. However, as IONP 5 was only cytotoxic to cancer cells (A549) that overexpress folate receptor, [15,16] it can be utilized as a potential targeted multifunctional (imaging and therapeutic) nanoagent for the treatment of folate-receptor-expressing tumors.

To further explore the potential biomedical applications of the synthesized functional PAA-IONPs, we evaluated the selective uptake of the folate-functionalized nanoparticle (4) by A549 lung cancer cells, as these cells overexpress the folate receptor. In these experiments, carboxylated (2) or folate-conjugated (4) nanoparticles (1.1 mg/mL) were incubated with A549 cells (10,000 cells) for 3 h, washed to remove non-internalized nanoparticles and visualized via confocal microscopy. Results showed no internalization of the carboxylated nanoparticle (2) as expected (Figure 3A, 3D). However, significant internalization of the folate-conjugated nanoparticle (4) was indicated by the presence of intense fluorescence in the cytoplasm of the cells (Figure 3B, 3E). These results were also observed in experiments performed using live (non-fixed) A549 cells, where internalization of the folate-decorated IONPs (4) was monitored through fluorescence microscopy (Supporting Information 11). The enhanced cellular uptake of the folate-decorated nanoparticle (4) in A549 cells may have been attributed to folate-receptor mediated internalization. As internalization of 4 was nominal in A549 cells pre-incubated with free folate and in studies using the H9c2 cardiomyocyte cell line (Supporting Information 12), we corroborated the receptor-mediated internalization of our folate-decorated IONPs (4). Next, we investigated the cellular uptake of a multifunctional folate-conjugated nanoparticle (5) with dual imaging and targeted cancer therapeutic properties. When these IONPs were incubated with A549 cells, mitotic arrest was observed, leading to dramatic cellular morphological changes and cell death (Figure 3C, 3F).

The therapeutic application of our nanoparticles depends on the rate of release of the encapsulated drug from the PAA coating. To evaluate 5's drug release profile, enzymatic (esterase) and low-pH degradation experiments were performed. Results indicated a fast release of the drug (Taxol) from the nanoparticle (5) upon esterase incubation, reaching a plateau within 2 hours (Figure 4A). An even faster release of the drug was observed at pH 4.0, reaching a plateau within 30 minutes (Figure 4B). No significant release of the drug was observed from nanoparticles incubated in PBS, pH 7.4. These results are significant as they demonstrate the stability of the nanoparticles during storage (PBS), and their cargo release only after cellular uptake via either esterase-mediated degradation or in acidified lysosomes. Therefore, only after its folate-receptor-mediated uptake, the nanoparticle 5 becomes cytotoxic upon intracellular release of its cargo therapeutic agent. Interestingly, a much slower release of the dye was observed, both upon esterase incubation and at pH 4.0 (Figure 4C and 4D). However, no release of the dye was observed at normal physiological pH (7.4).

The observed differential release of the drug vs. the dye from IONP 5 may be attributed to the drug's (Taxol) size and hydrophobic nature.

Taken together, these results make our folate-decorated-IONP (5) an important drug carrier, as it can rapidly release Taxol and therefore induce cell death only upon targeted cell internalization. Furthermore, the acidic microenvironment of most tumors could enhance the release of Taxol and dye from the nanoparticle into the tumor to facilitate the monitoring of tumor regression by MR and optical imaging. Also, by modifying the targeting moiety of the theranostic IONP's surface, other carcinomas may be targeted, while obtaining important spatiotemporal information for clinical decision making.

For *in vivo* imaging applications, nanoparticles with excitation and emission in the near infrared region (650–900 nm) are needed for deep tissue fluorescence imaging.[17] Towards this end, we encapsulated a near infrared dialkylcarbocyanine dye (DiR, excitation/emission: 751/780 nm) into the carboxylated (2-DiR) and folate-conjugated (4-DiR) IONPs, following the same synthetic protocol described for the synthesis of IONPs 2 and 4. UV/Vis studies corroborated the presence of the near infrared DiR dye within the nanoparticle's PAA coating (Supporting information 8b). To demonstrate the targeting capability of our functional near-infrared and folate-derivatized IONP (4-DiR) to folate receptor expressing cells and eventually assess their intracellular activity, we incubated A549 lung carcinoma cells with the (4-DiR) nanoparticle and imaged the cells using fluorescence imaging techniques.

In these studies, A549 cells (10,000 cells) were treated with either DiR-carrying carboxylated (2-DiR) or DiR-carrying folate-conjugated (4-DiR) IONPs (1.1 mg/mL) for 3 h. Next, the cells were washed with PBS and detached with trypsin. After centrifugation, the resulting cell pellets were simultaneously imaged using an indocyanine green (ICG) filter. No cell-associated near infrared fluorescence was observed in cells treated with the carboxylated (2-DiR) nanoparticles (Supporting Information 13A). In contrast, a dose-dependent cell-associated DiR fluorescence was observed in cells treated with the folate-conjugated (4-DiR) nanoparticles (Supporting Information 13B). Since the cells were extensively washed with PBS before imaging and considering the confocal microscopy results shown in Figure 3, it is plausible that the cells have internalized the (4-DiR) nanoparticles via folate-receptor-mediated endocytosis, thus endowing these cells with near infrared fluorescent. To further confirm the association of these nanoparticles with folate-expressing A549 carcinoma cells, the cells pellets were re-suspended in PBS and their fluorescence emission and MRI signal ( $T_2$  relaxation time) were recorded. As expected, an increase in fluorescence emission intensity and decrease in magnetic relaxivity ( $T_2$ ) was observed from the corresponding suspension of the cell pellets (Table 2). No fluorescence emission or  $T_2$  changes were observed in H9c2 cardiomyocytes treated with 4-DiR. Therefore, these results indicate that our targeted multimodal nanoparticles can simultaneously allow the near infrared fluorescence and MR imaging of folate-receptor expressing cells.

To further assess the utility of the multimodal nanoparticle 4 encapsulating either DiI (4-DiI) or DiR (4-DiR), fluorescence and MRI studies were performed. First, phantoms containing both nanoparticles in PBS were taken using a dedicated optical imaging animal scanner (Maestro, CIR, Woburn, MA). Results indicated the potential use of the 4-DiR nanoparticle for near infrared imaging, even in a nanoparticle suspension containing both 4-DiI and 4-DiR IONPs (Supporting Information 14A-E). These results are important as they point to the possibility of simultaneously imaging both nanoparticles, which could be utilized in the imaging of two different targets in *in vivo* experiments (e.g. 2 different cell populations). Furthermore, magnetic resonance imaging (MRI) studies of 4-DiI and 4-DiR nanoparticle

dilutions (Supporting Information 15) using a 4.7T MRI scanner (Bruker, Bellerica MA) further demonstrated the ability of these IONPs to behave as sensitive MRI contrast agents.

In conclusion, we introduce a new method to synthesize multimodal and theranostic PAA-IONPs for the potential *in vivo* target-specific detection and treatment of tumors. Our novel IONPs are biocompatible and biodegradable, as they are synthesized from biodegradable and biocompatible components. These functional IONPs are stable in aqueous buffered solutions, possess good cellular targeting ability, and their simple synthesis process is amenable to scale-up. In addition, this method can easily be used to generate libraries of targeted theranostic nanoparticles with different targeting ligands or encapsulated agents, and even include different metallic cores. Furthermore, the drug-encapsulating IONPs when conjugated with folic acid (using “click” chemistry) provide targeted drug delivery to cancer cells that overexpress the folate receptor, while avoiding normal cells that do not overexpress this receptor. We anticipate that this multimodal (magnetic and fluorescent) and multifunctional (imaging and therapeutic) IONPs will open many exciting opportunities for the targeted delivery of therapeutic agents to tumors. In addition, the dual optical and magnetic properties of the synthesized nanoparticles will allow for the dual fluorescence- and MR-based imaging and monitoring of drug efficacy. All these positive attributes make the functional IONPs a promising drug delivery vehicle for further *in vivo* evaluation.

## Experimental Section

### Synthesis of PAA-IONPs (1)

For the water-based, step-wise synthesis of polyacrylic acid-coated iron oxide nanoparticles (PAA-IONPs), three solutions were prepared; an *iron salt solution* [0.62 g of  $\text{FeCl}_3 \cdot 6\text{H}_2\text{O}$  and 0.32 g of  $\text{FeCl}_2 \cdot 4\text{H}_2\text{O}$  in dilute HCl solution (100  $\mu\text{L}$  of 12 N HCl in 2.0 mL  $\text{H}_2\text{O}$ )]; an *alkaline solution* [1.8 mL of 30 %  $\text{NH}_4\text{OH}$  solution in 15 mL of  $\text{N}_2$  purged DI water]; and a *stabilizing agent solution* [820 mg of polyacrylic acid in 5 mL of DI water]. To synthesize the PAA-IONP, the *iron salt solution* was added to the *alkaline solution* under vigorous stirring. The resulting dark suspension of iron oxide nanoparticles was stirred for approximately 30 seconds before addition of the *stabilizing agent solution* and stirred for 1 h. The resulting suspension of PAA-IONPs was then centrifuged at 4000 rpm for 30 minutes and the supernatant was washed three times with DI water to get rid of free polyacrylic acid and other unreacted reagents using an amicon 8200 cell (Millipore ultra-filtration membrane YM – 30 k). Finally, the PAA-IONP suspension was purified using magnetic column, washed with phosphate buffer saline (pH = 7.4) and concentrated using the amicon 8200 cell system. The iron concentration and magnetic relaxation of the PAA-IONPs was determined as previously reported [Josephson et. al. *Bioconjugate Chem.* 1999, 10, 186–191]. The successful coating of the IONPs with PAA was confirmed by the presence of a negative zeta-potential ( $\zeta = -48$  mV) and the characteristic acid carbonyl bands on the FT-IR spectroscopic analysis of the nanoparticles (Supporting Information 1 and 5).

### Synthesis of propargylated IONPs (3): Carbodiimide chemistry

To a suspension of PAA-IONP (1) (45 mg Fe) in MES buffer (26 mL, pH = 6), a solution of EDC (87 mg, 10 mmol) and NHS (52 mg, 10 mmol) in MES buffer (2 mL) was added and incubated for 3 minutes. To the resulting reaction mixture, propargyl amine (25 mg, 10 mmol) in DMF (0.5 mL) was added drop-wise and incubated for 5 h at room temperature. The resulting reaction mixture was then purified using magnetic column and then using amicon 8200 cell (Millipore ultra-filtration membrane YM – 30 k) to get rid of unreacted propargyl chloride and other unreacted reagents and kept in PBS at 4 °C. FT-IR data analysis (Supporting Information 6) confirms the completion and success of the conjugation.

### **General procedure for dye-encapsulated functional IONPs (2, 4): Modified solvent diffusion method**

To a suspension of IONPs (4.5 mL, [Fe] = 1.1 mg/mL) in PBS, a solution of the corresponding dialkylcarbocyanine fluorescent dyes (DiI or DiR, 0.1 µg/µL) in DMF was added drop-wise at room temperature with continuous stirring at 1000 rpm. The resulting dye-encapsulated IONPs were purified using magnetic column and then dialyzed (using 6–8 K molecular weight cut off dialysis bag) three times against deionized water and finally against phosphate buffered saline solution. The successful encapsulation of the corresponding dye (DiI or DiR) on the PAA-IONPs was confirmed by UV/Vis spectrophotometric measurements (Supporting Information 6a-b). In addition, when these nanoparticles were functionalized with folate, the presence of both folate and dye encapsulated groups were assessed by UV/Vis (Supporting Information 9a) and fluorescence (Supporting Information 9b) spectrometry.

### **Procedure for the co-encapsulation of Paclitaxel and DiI into IONPs (5)**

A solution containing paclitaxel (5 µL, 0.05 µg/µL) and DiI dye (5 µL, 0.1 µg/µL) in 500 µL DMF was used and the same modified solvent diffusion method was followed as described above. The presence of taxol in the IONPs (5) was confirmed by using fluorescence spectrophotometer (Supporting Information 10).

### **Synthesis of 3a: Folate conjugation using Click chemistry**

To a suspension of propargylated IONPs 3 (13 mg Fe) in bicarbonate buffer (pH = 8.5), a catalytic amount of CuI (0.06 µg,  $3 \times 10^{-10}$  mmol) were added for a total volume of 125 µL of bicarbonate buffer and vortexed for 30 seconds. Then, a solution of azide-functionalized folic acid (7, Supporting Information 2, 0.003 g,  $6 \times 10^{-2}$  mmol) in DMSO was added and incubated at room temperature for 12 h. The final reaction mixture was purified by using magnetic column and by dialysis using 6–8 K molecular weight cut off dialysis bag, against deionized water first and a finally with a phosphate buffered saline (PBS) solution. The purified functional IONPs were stored at 4 °C until further use. The successful conjugation of folic acid with PAA-IONPs was confirmed by UV/Vis (Supporting Information 7a) and fluorescence (Supporting Information 7b) spectrophotometric measurements.

### **Cell culture and cell viability studies: MTT assay**

The lung carcinoma cells (A549) and cardiomyocytes (H9c2) were obtained from ATCC, USA. Lung carcinomas were grown in Kaighn's modification of Ham's F12 medium (F12K – Cellgro), supplemented with 5% fetal bovine serum (Heat-inactivated FBS – Cellgro), L-glutamine, streptomycin, amphotericin B, and sodium bicarbonate. The cells were maintained at 37 °C, 5% CO<sub>2</sub> in a humidified incubator. Cardiomyocyte cells were grown in Eagle's Minimal Essential medium supplemented with 10 % fetal bovine serum, sodium pyruvate, L-glutamine, penicillin, streptomycin, amphotericin B and sodium bicarbonate. For MTT assay, lung carcinoma and cardiomyocyte cells (2,500 cells/well) were seeded in 96-well plates, and were incubated with the IONPs for 3 h at 37 °C. Then, each well was washed three times with 1X PBS and treated with 20 µL MTT (5 µg/µl, 3-(4,5-dimethylthiazol-2-yl)-2,5-diphenyltetrazolium bromide, Sigma-Aldrich ) for 2 h. The resulting formazan crystals were dissolved in acidified isopropanol (0.1 N HCl) and the absorbance was recorded at 570 nm and 750 nm (background), using a Synergy HT multi-detection microplate reader (Biotek). These experiments were performed in triplicates.

### **Cellular internalization: Confocal Microscopy and IVIS experiments**

A Zeiss LSM 510 confocal and Zeiss Axiovert 200 epifluorescence microscopes were used to assess the uptake of folate-derivatized IONPs by the human lung carcinoma (A549) cell

line. Specifically, A549 cells (10,000) were incubated with the corresponding IONPs preparation (1.1 mg/mL) for 3 h in a humidified incubator (37 °C, 5% CO<sub>2</sub>). Subsequently, the cells were thoroughly washed three times with 1X PBS and fixed with 10% formalin solution. Nuclear staining with DAPI was performed as recommended by the supplier. Then, multiple confocal images were obtained, achieving a representative view of the cell-IONPs interaction. For the IVIS analysis, 10,000 lung carcinoma cells were incubated for 3 h with the corresponding IONPs and the supernatant was collected in eppendorf tubes. Cells were thoroughly washed with 1X PBS and detached them, as stated above. The resulting pellets were resuspended in 1 mL culture media. All eppendorf tubes were examined simultaneously on a Xenogen IVIS system, using the ICG filter for DiR dye. All experiments were performed in triplicates.

### In Vitro drug/dye release

The *in vitro* drug/dye release studies were carried out using a dynamic dialysis technique at 37 °C. Briefly, 100 µL of IONPs (5) are incubated with a porcine liver esterase (20 µL) inside a dialysis bag (MWCO 6000–8000), which is then placed in a PBS solution (pH 7.4). The amount of guest (dye or drug) molecules released from the nanoparticle into the PBS solution was determined at regular time intervals by taking 1-mL aliquots from the PBS solution and measuring the fluorescence intensity at 581 nm for DiI and 375 nm for Taxol. The concentration of the either dye or drug was calculated using a standard calibration curve. The cumulative fraction of release versus time was calculated using the following equation:

$$\text{Cumulative release (\%)} = \frac{[\text{guest}]_t}{[\text{guest}]_{\text{total}}} \times 100$$

Where  $[\text{guest}]_t$  is the amount of guest released at time  $t$ ,  $[\text{guest}]_{\text{total}}$  is the total guest present in the guest encapsulated IONPs.

### Supplementary Material

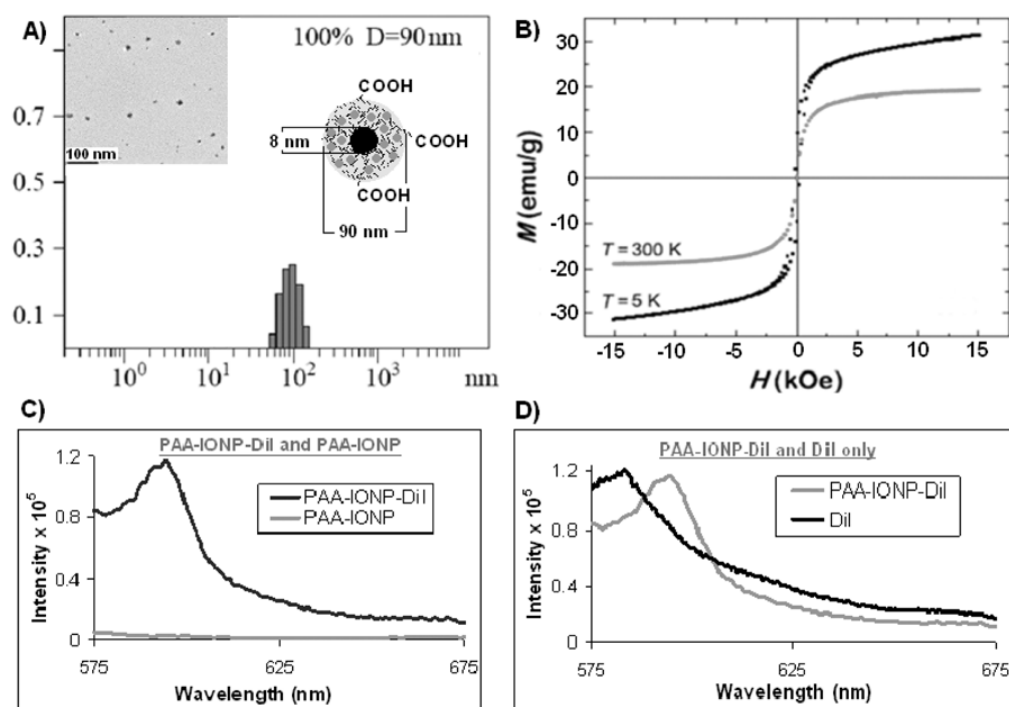
Refer to Web version on PubMed Central for supplementary material.

### References

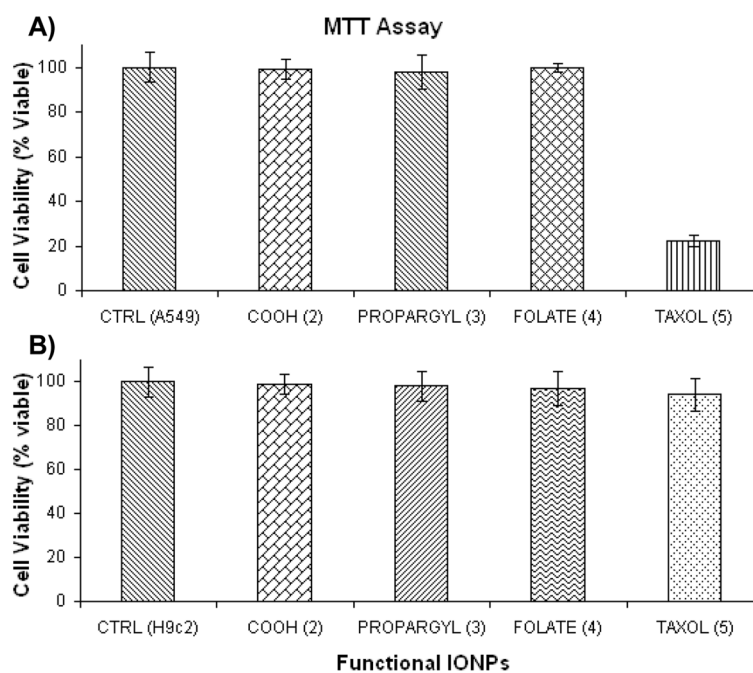
1. a) McCarthy JR, Kelly KA, Sun EY, Weissleder R. *Nanomedicine* 2007;2:153–167. [PubMed: 17716118] b) Gupta AK, Gupta M. *Biomaterials* 2005;26:3995–4021. [PubMed: 15626447]
2. Nasongkla N, Bey E, Ren J, Ai H, Khemtong C, Guthi JS, Chin SF, Sherry AD, Boothman DA, Gao J. *Nano Lett* 2006;6:2427–2430. [PubMed: 17090068]
3. a) Lewin M, Carlesso N, Tung CH, Tang XW, Cory D, Scadden DT, Weissleder R. *Nat Biotechnol* 2000;18:410–414. [PubMed: 10748521] b) Josephson L, Kircher MF, Mahmood U, Tang Y, Weissleder R. *Bioconjugate Chem* 2002;13:554–560. c) Weng KC, Noble CO, Papahadjopoulos-Sternberg B, Chen FF, Drummond DC, Kirpotin DB, Wang D, Hom YK, Hann B, Park JW. *Nano Lett* 2008;8:2851–2857. [PubMed: 18712930]
4. a) Choi JH, Nguyen FT, Barone PW, Heller DA, Moll AE, Patel D, Boppart SA, Strano MS. *Nano Lett* 2007;7:861–867. [PubMed: 17335265] b) Mulder WJ, Koole R, Brandwijk RJ, Storm G, Chin PT, Strijkers GJ, de Mello Donega C, Nicolay K, Griffioen AW. *Nano Lett* 2006;6:1–6. [PubMed: 16402777]
5. Yu MK, Jeong YY, Park J, Park S, Kim JW, Min JJ, Kim K, Jon S. *Angew Chem Int Ed Engl* 2008;47:5362–5365. [PubMed: 18551493]
6. Lee H, Yu MK, Park S, Moon S, Min JJ, Jeong YY, Kang HW, Jon S. *J Am Chem Soc* 2007;129:12739–12745. [PubMed: 17892287]



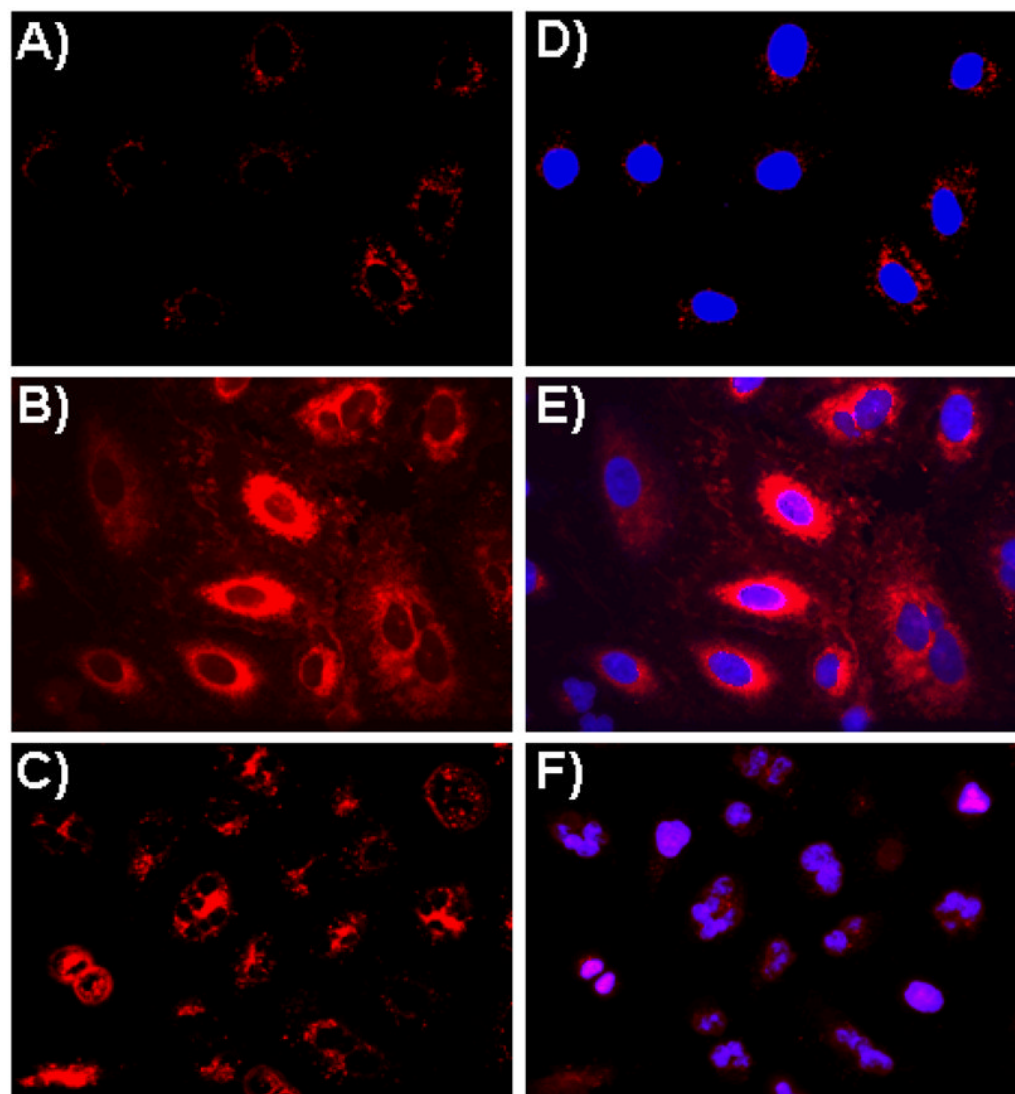
7. Lee H, Lee E, Kim do K, Jang NK, Jeong YY, Jon S. *J Am Chem Soc* 2006;128:7383–7389. [PubMed: 16734494]
8. Peng S, Wang C, Xie J, Sun S. *J Am Chem Soc* 2006;128:10676–10677. [PubMed: 16910651]
9. a) McCarthy JR, Perez JM, Bruckner C, Weissleder R. *Nano Lett* 2005;5:2552–2556. [PubMed: 16351214] b) Packard BS, Wolf DE. *Biochemistry* 1985;24:5176–5181. [PubMed: 4074686]
10. a) Sun EY, Josephson L, Weissleder R. *Molecular Imaging* 2006;5:122–128. [PubMed: 16954026] b) Kolb HC, Finn MG, Sharpless KB. *Angew Chem Int Ed Engl* 2001;40:2004–2021. [PubMed: 11433435] c) White MA, Johnson JA, Koberstein JT, Turro NJ. *J Am Chem Soc* 2006;128:11356–11357. [PubMed: 16939250]
11. a) Santra S, Liesenfeld B, Dutta D, Chatel D, Batich CD, Tan W, Moudgil BM, Mericle RA. *J Nanosci Nanotech* 2005;X:1–6. b) Riebeseel K, Biedermann E, Lser R, Breiter N, Hanselmann R, Mlhaupt R, Unger C, Kratz F. *Bioconjugate Chem* 2002;13:773–785.
12. Shi M, Wosnick JH, Ho K, Keating A, Shoichet MS. *Angew Chem Int Ed Engl* 2007;46:6126–6131. [PubMed: 17628481]
13. a) Koch AM, Reynolds F, Kircher MF, Merkle HP, Weissleder R, Josephson L. *Bioconjugate Chem* 2003;14:1115–1121. b) Shen T, Weissleder R, Papisov M, Bogdanov A Jr, Brady TJ. *Magn Reson Med* 1993;29:599–604. [PubMed: 8505895]
14. Parker N, Turk MJ, Westrick E, Lewis JD, Low PS, Leamon CP. *Anal Biochem* 2005;338:284–293. [PubMed: 15745749]
15. Yuan H, Miao J, Du YZ, You J, Hu FQ, Zeng S. *Int J Pharm* 2008;348:137–145. [PubMed: 17714896]
16. Nelson ME, Loktionova NA, Pegg AE, Moschel RC. *J Med Chem* 2004;47:3887–91. [PubMed: 15239666]
17. Weissleder R, Ntziachristos V. *Nat Med* 2003;9:123–128. [PubMed: 12514725]



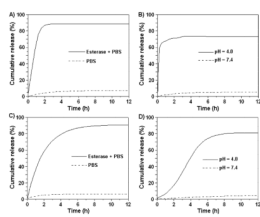
**Figure 1.** Characterization of multimodal nanoparticles 2 (PAA-IONP-DiI). A) Determination of hydrodynamic diameter of the IONPs through Dynamic Light Scattering (DLS), Inset: Transmission Electron Microscope (TEM) image of the corresponding nanoparticles. Scale bar 100 nm. B) magnetic hysteresis loops at 300 and 5 K, showing nanoparticles are superparamagnetic C) fluorescence emission spectra (in PBS buffer) of DiI dye encapsulated IONPs 2 and that of 1 without any dye, D) fluorescence emission spectra of 2 and that of free non-encapsulated DiI in solution.



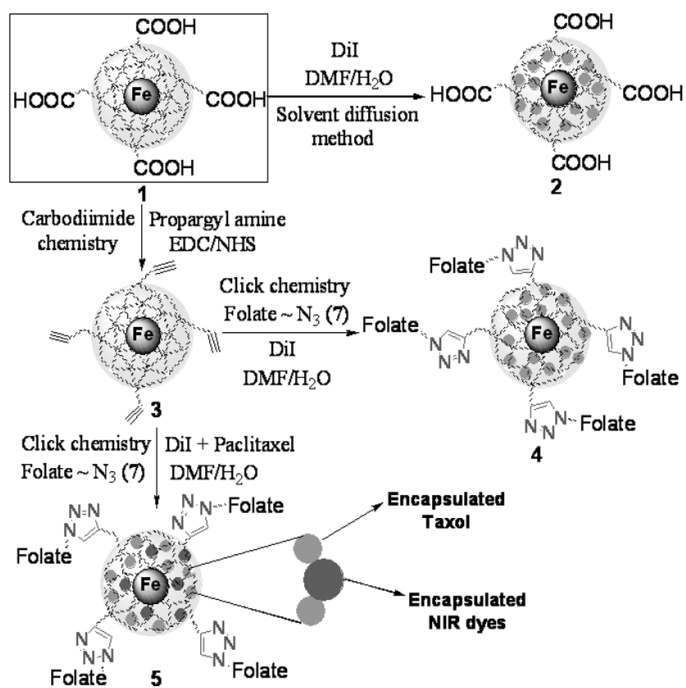
**Figure 2.** Determination of cytotoxicity of the functional IONPs: carboxylated [COOH (2)], propargylated [PROPARGYL (3)], folate-conjugated [FOLATE (4)] and Taxol-carrying [TAXOL (5)]. Control (CTRL) cells: A) Lung carcinoma cells (A549) and B) Cardiomyocyte cells (H9c2) were treated with PBS. Average values of four measurements are depicted  $\pm$  standard error.



**Figure 3.** Assessment of IONPs' cellular uptake via confocal laser-scanning microscopy using lung carcinoma A549 cells. A) No internalization was observed in cells treated with carboxylated IONPs (2), as no DiI fluorescence was observed in the cytoplasm, B) Enhanced internalization was observed upon incubation with the folate-immobilized IONPs (4), C) Cells incubated with Taxol and DiI co-encapsulating folate-functionalized IONPs (5) induced cell death. (D–F) Corresponding merged confocal images of the functional IONPs treated cells with their nucleus stained with DAPI (blue).



**Figure 4.** Drug and dye release profiles of functional IONPs (5) in PBS (pH = 7.4) at 37 °C. Release of Taxol (A & B) and DiI (C & D) were observed in the presence of an esterase enzyme (A & C) and at pH 4.0 (B & D).

**Scheme 1.**

Schematic representation of the synthesis of theranostics and multimodal IONPs. Click chemistry and carbodiimide chemistry have been used for the synthesis of a library of functional IONPs. Near IR dyes- and paclitaxel co-encapsulated IONPs were prepared in water using the modified solvent diffusion method (See Supporting Information 1 and 2 for detailed synthetic procedures).

**Table 1**

Determination of magnetic relaxivity ( $R_2$ ), hydrodynamic diameter (D) and polydispersity index (PDI) of functional IONPs immediately after synthesis. Quantitative estimation of amount of dye, folic acid and Taxol per iron crystal of the corresponding multifunctional IONPs (1–5).

IONPs	$R_2$ [ $s^{-1}mM^{-1}$ ]	D (PDI) [nm]	Dye/IONPs	Folate/IONPs	Taxol/IONPs
1	206 $\pm$ 2	86 (0.89) $\pm$ 1	-	-	-
2	202 $\pm$ 3	90 (0.87) $\pm$ 2	31 $\pm$ 2	-	-
3	207 $\pm$ 2	87 (0.89) $\pm$ 1	-	-	-
4	204 $\pm$ 3	94 (0.87) $\pm$ 3	28 $\pm$ 2	12 $\pm$ 2	-
5	203 $\pm$ 5	96 (0.91) $\pm$ 4	19 $\pm$ 1	12 $\pm$ 2	11 $\pm$ 3

**Table 2**

Determination of fluorescence emission intensity [a. u.] and magnetic relaxivity ( $T_2$ ) of IONP-(4-DiR)-treated cells (A.549) in PBS.

A549 Cell pellets	Cells only	Cells + 20 $\mu$ L IONPs	Cells + 40 $\mu$ L IONPs	Cells + 60 $\mu$ L IONPs	Cells + 80 $\mu$ L IONPs
Fl. Emission ( $\times 10^5$ )	0.0	1.7	2.0	2.4	2.7
$T_2$ [ms]	2000	165	126	101	78